THE JOURNAL OF PHYSICAL CHEMISTRY C LETTERS

2007, *111,* 16092−16095
Published on Web 10/16/2007

Selective Growth of Pure and Long ZnO Nanowires by Controlled Vapor Concentration Gradients

Samuel L. Mensah, Vijaya K. Kayastha, and Yoke Khin Yap*

Department of Physics, Michigan Technological University, 1400 Townsend Drive, Houghton, Michigan 49931

Received: August 8, 2007; In Final Form: September 24, 2007

ZnO can appear as nanowires, nanobelts, and nanocombs, which are attractive for various applications. However, this has prevented the growth of desired nanostructures without other trace morphologies. Here we demonstrated a mechanism for selective growth of pure and long ZnO nanowires. This was obtained by placing a gold film at a high-temperature zone so that ZnO nanowires with controllable densities can be grown on adjacent bare substrates at lower temperature zones. The concentration gradients of gold and ZnO vapors are responsible for this selective growth, which could be applicable for selective growth of ZnO nanobelts and nanocombs in the future.

ZnO nanostructures have proven to be promising materials for applications in electronics and optoelectric devices.[1−3] Their wide direct band group of 3.37 eV and strong exciton binding energy of 60 meV at room temperature are particularly attractive for electo-optical devices. ZnO nanostructures such as nanowires/nanorods,[3,4] nanobelts,[5] and nanocombs[6] that have been synthesized by various growth techniques and vapor-phase transport (thermal chemical vapor deposition) appear to be the simplest and most popular ones. ZnO nanowires (NWs) have exhibited interesting properties for electron field emission[7,8] and field effect transistors.[9,10] Short NWs (typically a few micrometers) have been commonly grown vertically aligned on substrates with high purity.[3,4] However, the growth of long ZnO NWs (>10 μm) by catalyst is always accompanied by traces of other nanostructures.[11] Here we defined a mechanism for selective growth of pure and long ZnO NWs by controlling the concentration gradients of the ZnO growth species and Au vapors. These long NWs could be used for fabricating multiple devices along each piece of NW. Results indicate that a similar approach could be applicable for the selective growth of other ZnO nanostructures in the future.

The growth of our ZnO nanostructures was performed in a horizontal furnace. This system consists of a quartz tube vacuum chamber. A smaller quartz tube (60 cm long and 2 cm in diameter) that contained the precursor materials and the substrates was placed within the vacuum chamber. A mixture of ZnO (0.2 g) and graphite (0.1 g) powder in an alumina boat was used as the precursor materials. These are placed at the closed end of the smaller quartz tube as shown in Figure 1a. Systematic experiments were carried out by placing a series of substrates (1 to 4) downstream from the precursor materials. The temperatures at the locations of these substrates were calibrated in a control experiment by inserting a thermocouple into the quartz tube. The small tube was then inserted into the vacuum chamber such that the closed end is at the center of the furnace. The temperature of the furnace was raised to 1100 °C at held for 30 min. At ∼350 °C, oxygen gas was introduced into the furnace at a desired flow rate from left to right side of Figure 1a. ZnO growth species were generated from the precursor materials and condensed on the substrates. Samples were analyzed by a scanning electron microscope (SEM), X-ray diffraction (XRD) using $CuK_{\alpha 1}$ radiation, transmission electron microscopy (TEM), Raman spectroscopy, and photoluminescence (PL).

In the first set of experiments, a series of oxidized Si substrates coated with 5-nm-thick Au films were used as shown in Figure 1a. Various ZnO nanostructures were formed at different oxygen flow rates. As grown by using 40 sccm of O_2 gas flows, ZnO films (b), wide nanobelts with trace NWs (c), NWs with trace nanobelts (d), and thick nanorods (e), were formed at ∼850 °C (substrate 1), ∼700 °C (substrate 2), ∼600 °C (substrate 3), and ∼500 °C (substrate 4), respectively. These experiments were repeated by a double flow rate of O_2 gas (80 sccm). In this case, ZnO films with bigger grain sizes (f), wide nanobelts with trace NWs (g), NWs with trace nanobelts (h), and nanocombs with trace nanobelts (i), were formed on substrate 1, 2, 3, and 4, respectively. Obviously, the formation of various ZnO nanostructures is possible but always mixed with various morphologies. In fact, NW samples with trace nanobelts (Figure 1d and h) can appear like pure and long NWs under SEM at low magnification.

In the second set of experiments, we are interested to understand the effects of the Au catalyst. We have put a series of oxidized Si substrates (without Au coatings) as shown in Figure 2a. In this case, formation of ZnO nanostructures solely by ZnO growth species will be revealed. We found that nothing was deposited on substrates located at temperatures higher than 750 °C. This can be explained by the excessive surface free energy and vapor pressures of ZnO growth species closer to the source materials. In this case, the probability of nuclei formation can be described as $P_N = A \exp(-\pi\sigma^2/k^2T^2In\alpha)$, where A is a constant, σ is the surface energy, $\alpha - 1$ is the supersaturation, $\alpha = p/p_o$, p is the pressure of vapor, p_o is the

* Corresponding author. E-mail: ykyap@mtu.edu.

10.1021/jp076382d CCC: $37.00

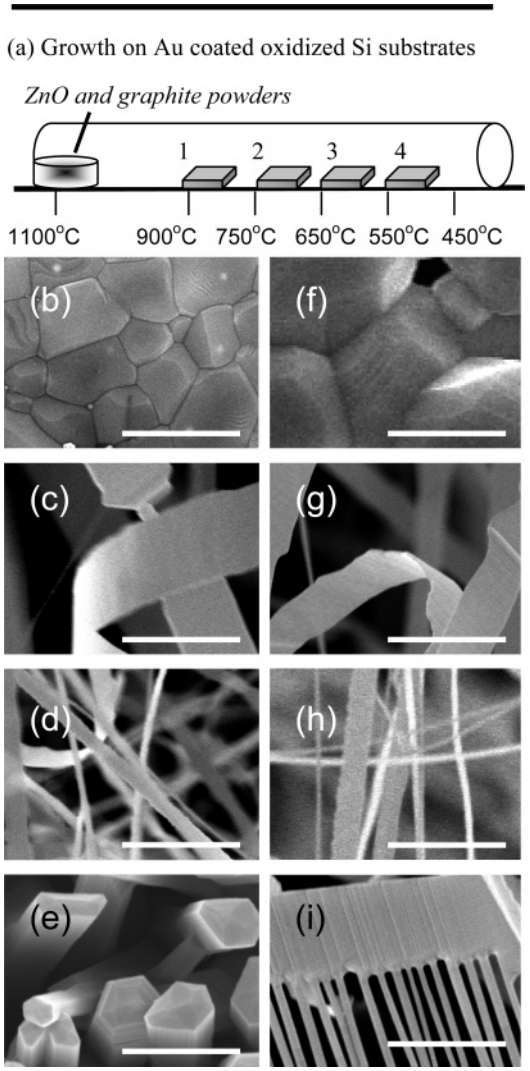

Figure 1. (a) Experimental setup for the growth with Au-coated substrates. ZnO (b) films, (c) wide nanobelts with trace NWs, (d) NWs with trace nanobelts, and (e) thick nanorods were formed on substrates 1, 2, 3, and 4, respectively, at O_2 gas flows of 40 sccm. ZnO (f) films with bigger grain sizes, (g) wide nanobelts with trace NWs, (h) NWs with trace nanobelts, and (i) nanocombs with trace nanobelts, were formed on substrates 1, 2, 3, and 4, respectively, at O_2 gas flows of 80 sccm. Scale bar = 1 μm.

equilibrium vapor pressure of the condensed phase at that temperature, k is the Boltzmann constant, and T is the temperature in Kelvin.[12] Relatively high σ will suppress the nucleation probability. Because ZnO films can be grown at ~850 °C with Au catalyst (Figure 1b and f), we interpret the function of Au as the catalyst to capture and condense ZnO vapors into solids. Figure 2 shows ZnO nanostructures grown without catalyst by using 40 sccm of O_2 gas flows. We detected ZnO (b) nanobelts with traces of NWs (substrate 1, ~700 °C), and (c), (d), (e) sharp-tip nanorods with varying diameters (~500−900 nm) and rod lengths (~8−15 μm) (substrates 2, 3, and 4 at ~600, ~500, and ~400 °C, respectively).

In the third set of experiments, we introduced a "side-catalyst" configuration as shown in Figure 3. Substrate 1 (~700 °C) was coated with a 5-nm Au film. Substrate 2 (~600 °C), substrate 3 (~500 °C), and substrate 4 (~400 °C) are oxidized Si substrates without Au coatings. The vapor transport mechanism of this configuration can be described by referring to Figure 4. As the temperature of the furnace (T) increases from T_1 to T_3,

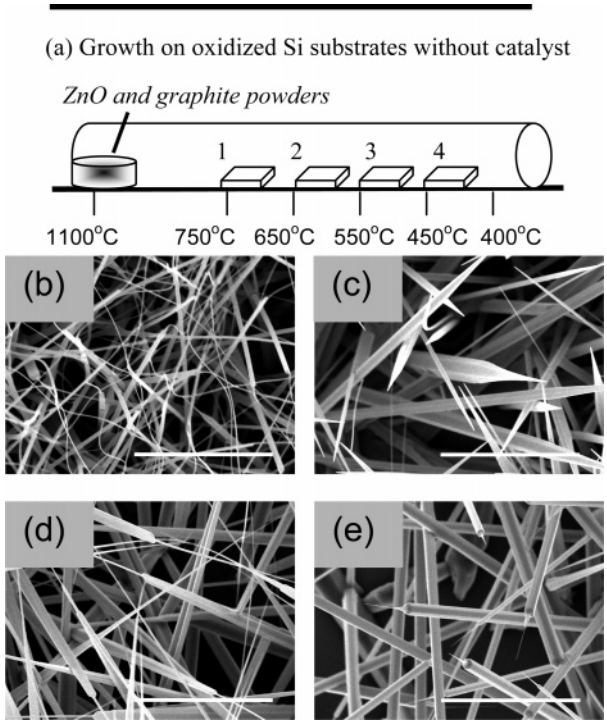

Figure 2. (a) Experimental setup for the growth without Au catalyst by using 40 sccm of O_2 gas flow. ZnO (b) nanobelts with traces of NWs, and (c), (d), (e) sharp-tip nanorods were grown on substrates 1, 2, 3, and 4, respectively. Scale bar = 6 μm.

the ZnO vapors will start to diffuse and propagate toward the substrates. Concurrently, the Au film on substrate 1 will start to evaporate because of the volatile near-surface atoms of the Au nanoparticles at high temperatures (melting point of bulk Au is 1064.43 °C but is lower for thin films and nanoparticles). According to Fick's law, the diffusion flux $J = -D(\mathrm{d}N/\mathrm{d}x)$, where J is the net flux of vapors (per unit area in unit time), D is the diffusion constant, and $(\mathrm{d}N/\mathrm{d}x)$ is the concentration gradients of the vapors along the propagation direction x.[13] This means that the diffusion will always propagate to a region with lower Au and ZnO vapor concentration as shown in Figure 4. Thus, this configuration will create concentration gradients of ZnO and Au vapors with higher concentration on substrate 1 and lowest concentration at substrate 4.

Results indicate that this approach leads to selective growth of pure ZnO NWs. For example, at 40 sccm of oxygen flows, short nanorods are formed in the Au-coated substrate (Figure 3b). This is different from those grown at substrate 2 in Figure 1a because of a much lower Au vapor concentration in the growth ambient because only one Au-coated substrate was used. Long ZnO NWs (~10 to 100s μm with diameters ~80 to 500 nm) were grown on substrates 2, 3, and 4 (Figure 3c, d, and e, respectively, or Figure 3f, g, and h, respectively, at lower magnification). NWs on substrates 2 and 4 have sharp tips but are much longer and smaller in diameter than the nanorods shown in Figure 2. NWs on substrate 3 have the longest lengths and more uniform diameters probably because of the optimum Au and ZnO vapor concentrations. Furthermore, the density of these NWs is controllable, higher on substrate 2 and lower on substrate 4. Apparently, Au vapors have mediated the growth of longer NWs, without which ZnO vapors will simply condense as short ZnO nanorods.

Typical XRD spectra of these ZnO NWs are shown in Figure 5a and can be indexed as wurtzite ZnO crystals (a = 0.325 nm and c = 0.521 nm). The dominant (002) peak indicates that

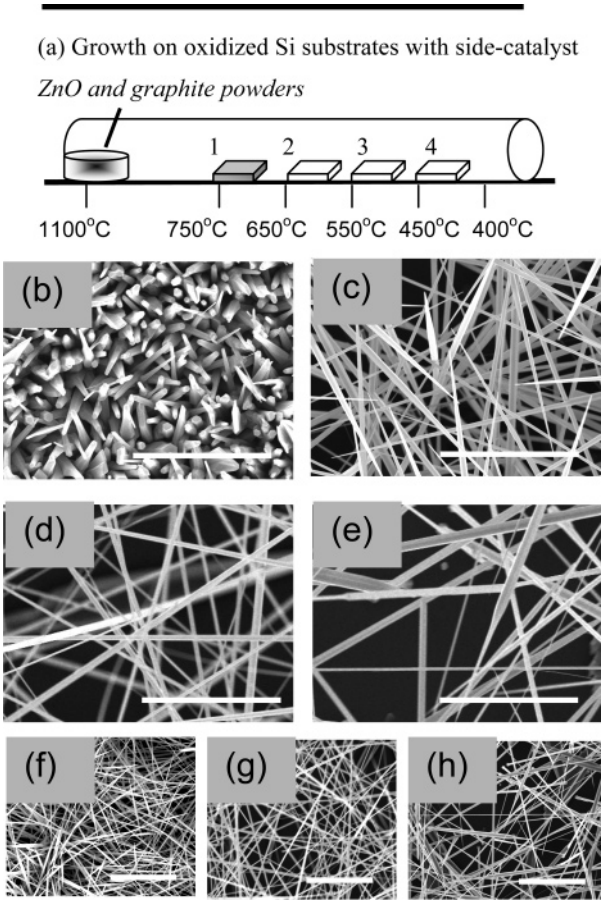

Figure 3. (a) Experimental setup for the growth with a side-catalyst by using 40 sccm of O_2 gas flow. ZnO (b) nanrods and NWs (c, d, and e) were grown on substrates 1, 2, 3, and 4, respectively. Scale bar = 6 μm. Low magnification of ZnO NWs on substrates 2, 3, and 4 are shown in f, g, and h, respectively. Scale bar = 10 μm.

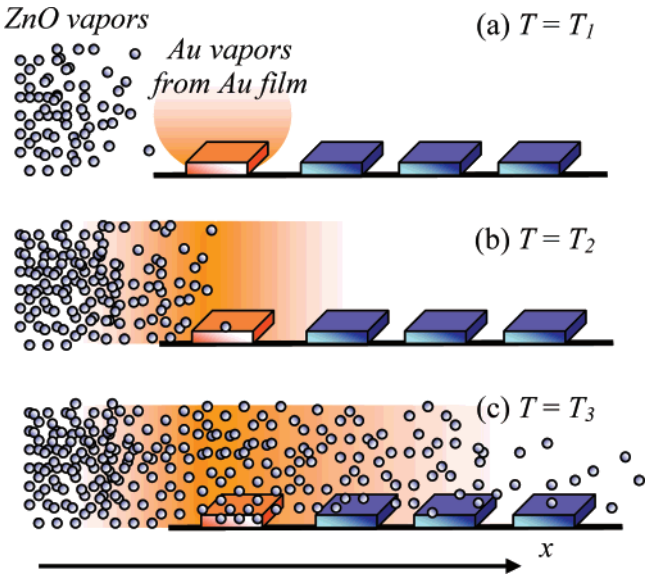

Figure 4. Schematic drawing of the diffusion of ZnO and Au vapors at various temperatures (a, b, and c), where $T_1 < T_2 < T_3$.

these NWs are grown along the *c* axis as confirmed by high-resolution TEM (inset). TEM also suggests that these ZnO NWs are single crystalline. Raman spectra of these ZnO NWs as excited by a HeNe laser (wavelength = 632.8 nm) indicate phonon frequencies at 331, 380, 438, and 581 cm^{-1}, which correspond to the $E_{2H} - E_{2L}$, A_{1T}, E_{2H}, and E_{1L} phonon modes

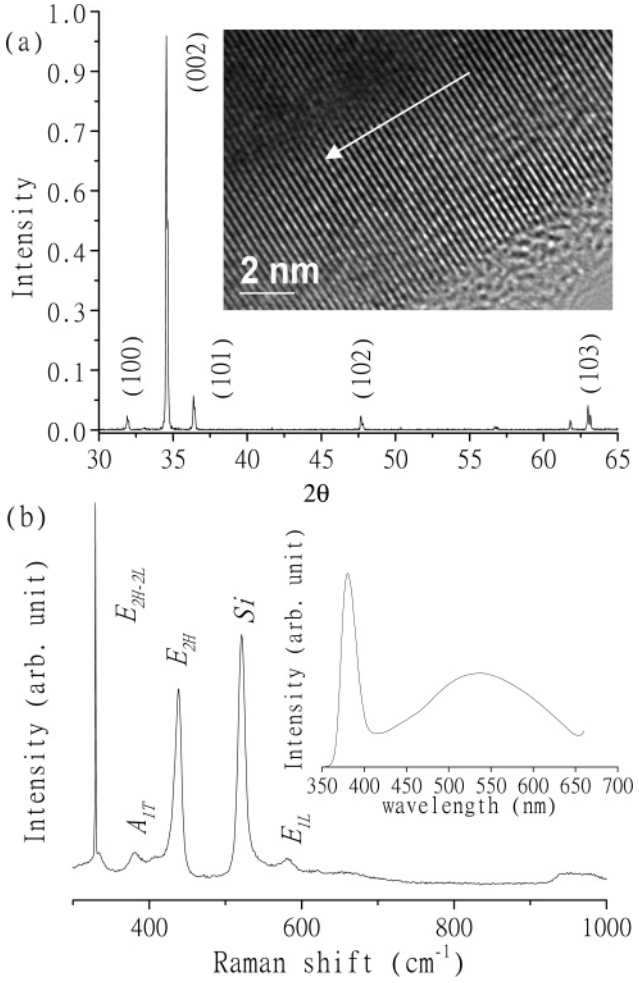

Figure 5. (a) XRD and HRTEM (inset, arrow = wire axis), (b) Raman and PL (inset) spectra of pure ZnO NWs.

of ZnO (Figure 5b).[14] These samples were also analyzed by PL as excited by a HeCd laser (wavelength ~325 nm). A predominant emission peak at ~380 nm is observed and corresponds to the near-band-edge emission of ZnO attributed to the recombination of the free excitons (inset in Figure 5b). A broad emission at ~530 nm is attributed to the recombination of a photogenerated hole with an electron occupying the oxygen vacancy.[14]

In summary, we have demonstrated selective growth of single-crystalline ZnO NWs by a side-catalyst configuration. The mechanism of this success is the introduction of controlled concentration gradients of ZnO and Au vapors. We believed that a similar mechanism could be applicable to control Au and ZnO vapors for selective growth of other ZnO nanotructures.

Acknowledgment. We acknowledge support from the U.S. Department of Army (Grant No. W911NF-04-1-0029, through the City College of New York), Defense Advanced Research Agency (Contract No DAAD17-03-C-0115, through Army Research Laboratory), and the Center for Nanophase Materials Sciences sponsored by the Division of Materials Sciences and Engineering, U.S. Department of Energy (Contract No DE-AC05-00OR22725 with UT-Battelle, LLC.).

References and Notes

(1) Arnold, M.; Avouris, P.; Pan, Z. W.; Wang, Z. L. *J. Phys Chem.* **2003**, *B107*, 659.

(2) Ng, H. T.; Han, J.; Yamada, T.; Nguyen, P.; Chen, Y. P.; Meyyappan, M. *Nano Lett.* **2005**, *4*, 1247.

(3) Huang, M. H.; Mao, S.; Feick, H.; Yan, H.; Wu, Y.; Kind, H.; Weber, E.; Russo, R.; Yang, P. *Science* **2001**, *292*, 1897.
(4) Li, Y.; Meng, G. W.; Zhang, L. D.; Philip, F. *Appl. Phys. Lett.* **2000**, *76*, 2011.
(5) Pan, Z. W.; Dai, Z. R.; Wang, Z. L. *Science* **2001**, *291*, 1947.
(6) Yan, H.; He, R.; Johnson, J.; Law, M.; Saykally, R. J.; Yang, P. *J. Am. Chem. Soc.* **2003**, *125*, 4728.
(7) Lee, C. J.; Lee, T. J.; Lyu, S. C.; Zhang, Y.; Rich, H.; Lee, H. J. *Appl. Phys. Lett.* **2002**, *81*, 3648.
(8) Jo, S. H.; Lao, J. Y.; Ren, Z. F.; Farrer, R. H.; Baldaccchini, T.; Fourkas, J. T. *Appl. Phys. Lett.* **2003**, *83*, 4821.
(9) Li, Q. H.; Wan, Q.; Liang, Y. X.; Wang, T. H. *Appl. Phys. Lett.* **2004**, *84*, 4556.
(10) Fan, Z.; Wang, D.; Chang, P.-C.; Tseng, W.-Y.; Lu, J. G. *Appl. Phys. Lett.* **2004**, *85*, 5923.
(11) Wang, Y. W.; Zhang, L. D.; Wang, G. Z.; Peng, X. S.; Chu, Z. Q.; Liang, C. H. *J. Cryst. Growth* **2002**, *234*, 171.
(12) Blakely, J. M.; Jackson, K. A. *J. Chem. Phys.* **1962**, *37*, 428.
(13) Kittel, C. *Introduction to Solid State Physics*, 6th ed; Wiley: New York, 1986; p 518.
(14) Mensah, S. L.; Kayastha, V. K.; Ivanov, I. N.; Geohegan, D. B.; Yap, Y. K. *Appl. Phys. Lett.* **2007**, *90*, 113108.